land

MDPI

Article

Construction of Long-Term Grid-Scale Decoupling Model: A Case Study of Beijing-Tianjin-Hebei Region

Xvlu Wang [1,2], Minrui Zheng [3,4,*], Dongya Liu [1], Peipei Wang [1], Xinqi Zheng [1,5,6], Yin Ma [7], Feng Xu [1], Xiaoyuan Zhang [1] and Tongshuai Rong [8]

[1] School of Information Engineering, China University of Geosciences (Beijing), Beijing 100083, China; wangxvlu@email.cugb.edu.cn (X.W.); zhxiaoyuan1997@email.cugb.edu.cn (X.Z.)
[2] Frontiers Science Center for Deep-Time Digital Earth, China University of Geosciences (Beijing), Beijing 100083, China
[3] School of Public Administration and Policy, Renmin University of China, Beijing 100872, China
[4] Digital Government and National Governance Lab, Renmin University of China, Beijing 100872, China
[5] Technology Innovation Center for Territory Spatial Big-Data, Ministry of Natural Resources of the People's Republic of China, Beijing 100036, China
[6] Observation and Research Station of Beijing Fangshan Comprehensive Exploration, Ministry of Natural Resources, Beijing 100083, China
[7] China Aero Geophysical Survey and Remote Sensing Center for Natural Resources, China Geological Survey, Beijing 100083, China
[8] Yantai Laiyang Environmental Monitoring Center (Yantai), Yantai 265200, China
* Correspondence: minruizheng@ruc.edu.cn

Abstract: Against the backdrop of rapid global economic development, the Beijing-Tianjin-Hebei (BTH) region, a pivotal economic hub and environmentally sensitive area in China, faces significant challenges in sustaining its landscape ecosystem. Given the region's strategic importance and vulnerability to environmental pressures, this study investigated the intricate relationships between landscape ecological risk, urban expansion, and economic growth (EG) in the BTH region. Utilizing the landscape as the focal point, we constructed a decoupling model at the grid scale to explore the decoupling relationship between the landscape ecological risk index (ERI), construction area growth (CAG), and EG. The results showed that (1) distinct stages and regional disparities were observed in the trends of ERI, CAG, and EG within the BTH region. The hot and cold spot patterns for these factors did not align consistently. (2) From 1995 to 2019, the coupling relationship between ERI, CAG, and EG in the BTH region underwent a fluctuating transition, initially moving from an undesirable state to an ideal state, and subsequently reverting to an undesirable state. Although the overall trends in these relationships showed some convergence, there were notable spatial distribution differences. (3) The spatial heterogeneity of the two decoupling relationships in the BTH region was relatively poor. Further analysis revealed that the evolution of these decoupling relationships was closely intertwined with regional policy shifts and adjustments.

Keywords: decoupling model; grid scale; landscape ecological risk index; change in construction land area; long-term sequence

check for updates

Citation: Wang, X.; Zheng, M.; Liu, D.; Wang, P.; Zheng, X.; Ma, Y.; Xu, F.; Zhang, X.; Rong, T. Construction of Long-Term Grid-Scale Decoupling Model: A Case Study of Beijing-Tianjin-Hebei Region. *Land* **2024**, *13*, 1853. https://doi.org/10.3390/land13111853

Academic Editor: Mário Gabriel Santiago dos Santos

Received: 23 September 2024
Revised: 24 October 2024
Accepted: 4 November 2024
Published: 6 November 2024

Copyright: © 2024 by the authors. Licensee MDPI, Basel, Switzerland. This article is an open access article distributed under the terms and conditions of the Creative Commons Attribution (CC BY) license (https://creativecommons.org/licenses/by/4.0/).

1. Introduction

With rapid economic growth (EG) and urbanization, the demand for construction land (CL) has increased significantly [1,2], leading to profound impacts on natural landscapes [3]. This trend results in the destruction of the natural environment and may elevate the landscape ecological risk index (ERI) [4,5]. Balancing the relationship between EG and landscape pattern changes to foster sustainable regional development has emerged as a pivotal research topic [6,7]. Understanding the transformation of the relationship between landscape patterns and economic growth across different periods is crucial to address this challenge. Existing research highlights the profound influence of EG and urbanization on

natural landscapes [8]. However, quantifying these impacts scientifically and exploring their underlying mechanisms poses significant challenges. To address these challenges, the introduction of evaluation models is particularly crucial to quantify these impacts more scientifically.

ERI is a comprehensive assessment model that provides a scientific basis for understanding the protection of ecosystem functions and health [9,10]. The ERI model evaluates the degree of the impact of external pressure on landscape ecosystems [11]. At present, source-sink and landscape pattern index methods are the primary methods for assessing ecological risks in landscapes. However, the overall evaluation of the former is relatively limited, and the landscape pattern index method can quantitatively express the structure and function of ecosystems. The landscape pattern index method has been widely used in this field. For instance, Shi et al. (2024) constructed a landscape ecological risk assessment model based on a landscape pattern index to assess spatial and temporal changes in ecological risk [12]. Cheng et al. (2023) assessed the characteristics of spatial and temporal changes in watershed landscape ecology using the same method [13]. Given its ability to fully reflect landscape structure and functional stability, this study adopted the landscape pattern index method to assess ERI.

After assessing landscape ecological risks, we needed to accurately quantify the relationship between landscape patterns and EG. The Tapio decoupling model offers new perspectives [14]. The Tapio decoupling model overcomes the difficulties of the traditional OECD decoupling model in selecting a base period. It improves measurement accuracy by introducing an elasticity coefficient to measure the decoupling between variables [15]. The model analyzes the overall decoupling status and local changes in detail, categorizing decoupling into types such as strong, weak, and expansionary negative decoupling, allowing for precise variable relationship descriptions. Consequently, decoupling models have been widely used. Applications include exploring the relationships between carbon emissions [16], urban CL expansion [17], energy consumption [18], water resource depletion [19], and economic development. Therefore, we used the Tapio decoupling model to quantify the relationship between the changes in landscape patterns and EG.

Considering the influence of scale effects on research, we investigated scale-related studies of decoupling applications. Decoupling analysis was mostly conducted based on short-term periods and administrative units as carriers [20], which could introduce biases due to varying resource elements within differently sized units [21]. To overcome these limitations, a grid-scale approach was adopted. This method transcends administrative boundaries, directly presents geographical unit-based results, facilitates the identification of anomalous regions, and enables deeper exploration [22,23]. Currently, there are few studies that have used the grid scale as a carrier and the "Five-Year Plan" as a stage to explore long-term decoupling relationships. In view of this, we conducted a long-term decoupling study at the grid scale to accurately detect the coupling relationship between pattern changes and EG.

The economic scale and vitality of the Beijing-Tianjin-Hebei (BTH) region have a significant nationwide influence. However, with rapid EG, the area of the CL has continued to increase, causing land and resource scarcity, intensified ecological and environmental pressure, and a significant impact on landscape ecological patterns [24]. This has increased the pressure on the ecological environment in the BTH region, reducing its carrying capacity for sustainable development. Therefore, it is crucial to explore effective strategies for managing landscape ecological risks while ensuring EG and rational planning to restrict uncontrolled expansion of CL. Many scholars have extensively studied the BTH region, focusing on profound changes in ERI, construction area growth (CAG), and EG [25–27]. However, most studies have focused on portraying the singular dimensions of EG trends, landscape ecological risk phenomena, or construction expansion [28] without a comprehensive understanding of the intricate interaction mechanisms among these factors [29,30]. This limits the accurate identification of key contradictions between socio-economic development and ecological pressures and hinders the formulation of scientific economic development plans

and environmental protection measures in the BTH region [31]. Therefore, this study selected CAG as an important driving force for changing the landscape ecological pattern [32] and the ERI as a measure reflecting the degree of impact on landscape ecology [33]. By studying the relationship among ERI, CAG, and EG, we measured the impact of regional EG on the landscape ecological environment.

This study used the BTH region as the research area and constructed an analytical framework for the decoupling relationship between the ERI, CAG, and EG at the grid scale. It analyzes the balance and conflict points between regional landscape pattern changes and EG from a long-term perspective. This study aims to dynamically and systematically reveal the coupling process between ERI, CAG, and EG in the BTH region and to understand the complexity and dynamics of their interactions. The results provide decision support and practical guidance for the BTH region to realize integrated high-quality development and promote the harmonious coexistence of the ecological environment and economy. This study raises the following questions: (1) How can the impact of EG on the landscape ecological environment be effectively quantified? (2) How can a decoupling model be constructed scientifically at the grid scale? (3) What type of coupling relationship and change mechanisms exist between ERI, CAG, and EG in the BTH region?

2. Materials and Methods

2.1. Study Area

The BTH region includes Beijing (core), Tianjin (key support), and Hebei (substantial hinterland) (Figure 1). According to the Collaborative Development Planning Outline for BTH, this region centers on the Bohai Rim transportation corridor, with Beijing and Tianjin as the cores and Xiong'an New Area as the new engine, spanning approximately 216,000 km^2 in Beijing, Tianjin, and Hebei. Since the implementation of the BTH collaborative development strategy in 2014, the gross domestic product (GDP) of the region reached 10 trillion yuan in 2022, 1.8 times that in 2013. By 2018, the area of CL had increased to 113 million mu, and the urbanization rate had reached 69.4% (National Bureau of Statistics, 2023).

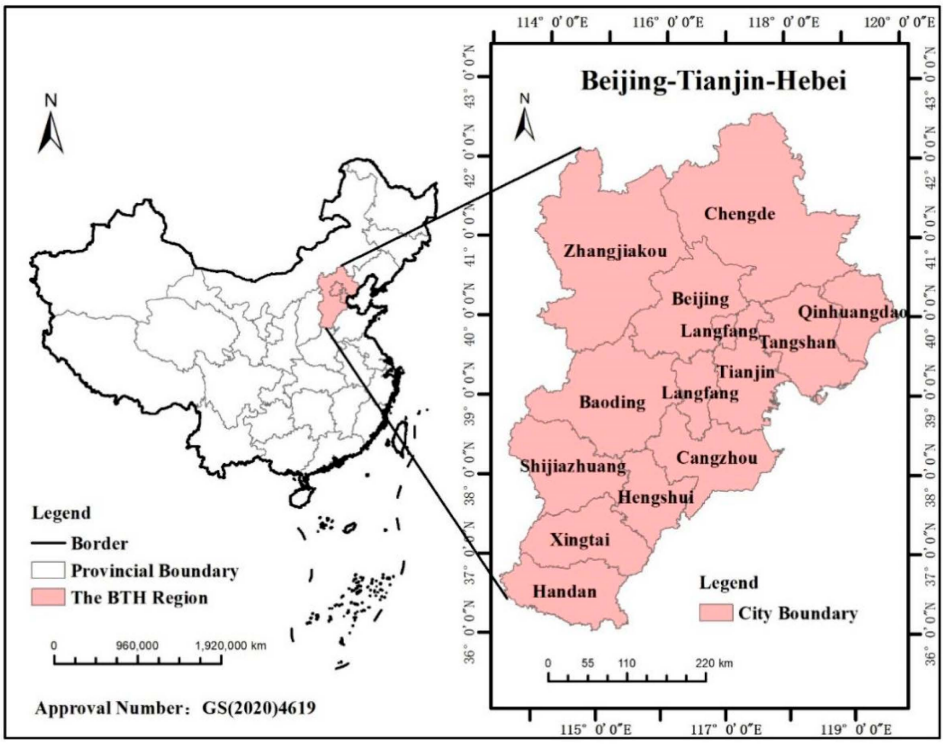


Figure 1. The map of the study area.

Despite its rapid EG and accelerated urbanization, the BTH region faces numerous challenges. Resource and environmental constraints tightened, highlighting issues such as water scarcity, air pollution, soil degradation [34], and intensified human-land conflicts due to a sharp imbalance between land supply and demand, limiting urban expansion [35]. Recently, while promoting high-quality economic development, the BTH region has intensified its ecological protection efforts and explored green development pathways. However, in the face of complex regional issues and challenges, in-depth research on the interaction mechanisms between the ERI, CAG, and EG in the BTH region is urgently needed [8]. Exploring the evolution of these coupled relationships could provide a scientific foundation and decision support for optimizing and regulating regional social ecosystems.

2.2. Data and Data Processing

This study focused on the BTH region by exploring the decoupling relationship between the ERI, CAG, and EG. Multi-period land use and GDP grid data were utilized. Given the lagged relationship between landscape changes, CAG, and EG, certain periods were adopted for the decoupling analysis. For period selection, the "Five-Year Plan" intervals in China's national economic planning (national economic planning is conducted every five years, such as 2001–2005) were referenced to ensure data timeliness and continuity. Consequently, six pivotal time nodes were selected for the analysis: 1995, 2000, 2005, 2010, 2015, and 2019. The selected periods correspond to different five-year plan periods or transition periods, such as 1995, which was on the eve of the "Ninth Five Year Plan" (1996–2000), when China's economy was in a critical period of transition from a planned economy to a market economy. At this time, the country began to pay more attention to the quality and efficiency of EG, as well as optimizing its economic structure. The selection of these time points helped us gain a deeper understanding and analysis of the development trajectory and trends of China's economy and policies during different periods. Since 2020, which marked the beginning of the COVID-19 pandemic, subsequent data lacked representativeness and were not considered in this study.

Regarding land use data, this study adopted 30 m resolution raster land use data [36]. To align with the research objectives, we reclassified the land types into forest land, grassland, water areas, cultivated land, CL, and unused land. For CL areas, identification was calculated based on grid ranges. For economic data, we used GDP grid data [37]. To ensure the accuracy and comparability of the data, we conducted preprocessing tasks, such as projection, clipping, and reclassification to match the grid data. Through strict selection of data sources and meticulous data processing, this study provides a solid data foundation for subsequent decoupling analyses. The details of the data sources are listed in Table 1.

Table 1. Data sources.

Data Type	Data Introduction	Download URL
land use data	These data achieved an overall accuracy of 80%, especially in the identification of forest land, water areas, and impervious surfaces. Its precision surpassed comparable products and could meet the research needs.	https://zenodo.org/records/5816591 (accessed on 5 June 2023)
GDP	GDP grid data released by the Resource and Environmental Science and Data Center of the Chinese Academy of Sciences, with a resolution of 1 km.	https://www.resdc.cn/DOI/DOI.aspx?DOIID=33 (accessed on 7 June 2023)

2.3. Method

To quantify the coupling between EG and landscape changes, a grid-scale decoupling model was constructed to precisely identify the areas of change. A long-term decoupling analysis was conducted on the EG, ERI, and CAG relationships in the BTH region. Furthermore, this study analyzes the spatiotemporal evolution and heterogeneity of the decoupling outcomes, as illustrated in Figure 2.

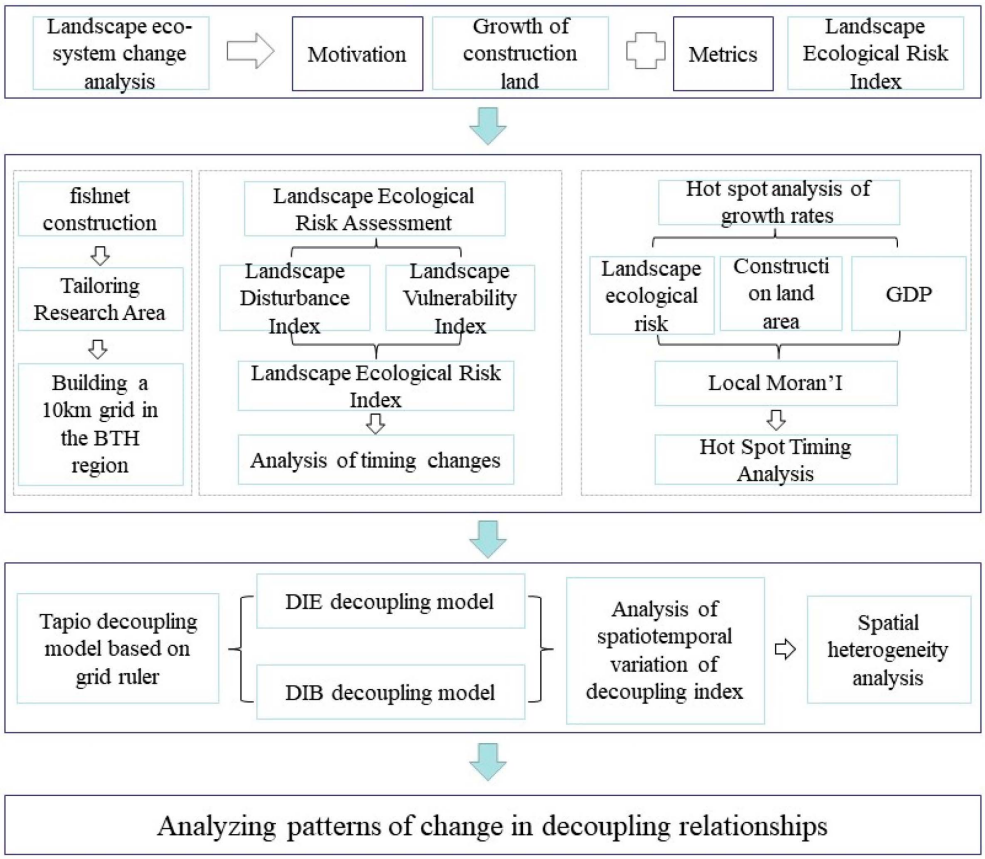


Figure 2. Research Framework.

2.3.1. Construction of Grids

Grids, a GIS technology, integrate geographical spatial resources through grid units and transcend traditional administrative boundaries for precise geographical analyses. Grids were constructed to capture the relationship between landscape patterns and EG in the BTH region. Referencing the relevant multi-scale research [38] and considering regional characteristics without losing grid scale detail [39], a 10 km × 10 km grid evaluation unit was selected. Marginal grids with disproportionately small areas were excluded to maintain geographical representation, resulting in 2253 valid grids.

2.3.2. Landscape Ecological Risk Analysis Model

The Landscape ERI evaluates ecological risks stemming from landscape patterns caused by human activities or external disturbances. This indicator couples human activities with ecological risks and serves as an important measure of changes in landscape ecology [30]. Therefore, landscape pattern indices related to landscape structure have been selected to quantify landscape ecological risks [12]. The landscape disturbance index (S_i) was calculated based on factors such as landscape fragmentation index (C_i), landscape separation index (D_i), and landscape dimension index (F_i). The comprehensive landscape disturbance index (S_i) and landscape vulnerability index (E_i) are used to obtain the landscape ERI. The specific formulas for the landscape pattern indices are presented in Table 2. The landscape ERI can be represented as follows:

$$ERI_k = \sum_{i=1}^{n} \frac{A_{ki}}{A_k} \times S_{ki} \times E_i \quad (1)$$

where ERI_k represents the ecological risk value of the kth grid; n denotes the number of different landscapes; i refers to the ith landscape type in the study area; A_{ki} represents

the area of landscape type i in the kth grid (ha^2); A_k is the total area of the kth grid (ha^2); S_{ki} indicates the degree of landscape disturbance of landscape type i in the kth grid; and E_i represents the landscape vulnerability of the ith landscape.

Table 2. Landscape Pattern Indices and their Ecological Significance.

Indices	Formula	Parameter Interpretation and Ecological Significance
Landscape disturbance index (S_i)	$S_i = aC_i + bD_i + cF_i$	It assesses the resistance of various landscape ecosystems to external disturbances [40]. C_i, D_i, and F_i represent the landscape fragmentation index, landscape separation index, and landscape dimension index of landscape type i, respectively. As the weights of the above three indices, referring to existing studies, a, b, and c are set as 0.5, 0.3, and 0.2, respectively [41]. To avoid the influence of different dimensions, the results of the above three landscape indices have been normalized.
Landscape Vulnerability Index (E_i)	E_i refers to relevant research [42], obtained through normalization	It represents the sensitivity of various landscape types to external disturbances, such as human activities and natural disasters, when their ecosystems are exposed [43]. Using the expert scoring method, different land use types are assigned values and normalized as follows: unused land = 6, water area = 5, cultivated land = 4, grassland = 3, forestland = 2, and construction land = 1 [44].
Landscape fragmentation index (C_i)	$C_i = \frac{n_i}{A_i}$	It indicates the degree of fragmentation in the landscape ecosystem following external disturbances [45]. n_i is the number of patches in landscape type i; A_i is the area of landscape type i. With a constant A_i, a higher number of patches within landscape type i results in a greater fragmentation index, indicating a more fragmented landscape.
Landscape Separation Index (D_i)	$D_i = \frac{1}{2} \times \sqrt{\frac{n_i}{A}} \times \frac{A}{A_i}$	It reflects the degree of spatial dispersion of a certain landscape patch [46]. A represents the total area of each landscape type, n_i is the number of patches in landscape type i, and A_i is the area of landscape type i.
Landscape Dimension Index (F_i)	$F_i = \frac{2\ln \frac{P_i}{4}}{\ln A_i}$	It reflects the degree of shape change in landscape patches following external disturbances [47]. P_i represents the perimeter of landscape i within the study area; and A_i is the area of landscape type i.

2.3.3. Decoupling Model Based on Grid

"Decoupling" describes the disappearance of the relationship between two or more previously correlated relationships, signifying a reduction in their mutual dependency, influence, or causality [48]. The Tapio decoupling model has the advantage of dynamism, is unaffected by changes in dimensions, and classifies decoupling states into eight categories (Table 3) [49]. However, research based on administrative divisions can limit the true spatial reflection of the Tapio decoupling model. Therefore, a grid-scale decoupling model was proposed to preserve the advantages of the model while overcoming administrative boundary constraints, enabling swift and precise identification of "abnormal" areas. The formulae are as follows:

$$DIE_k = \frac{(ERI_{kt} - ERI_{kt-1})/ERI_{kt-1}}{(GDP_{kt} - GDP_{kt-1})/GDP_{kt-1}} = \frac{\Delta ERI}{\Delta GDP} \quad (2)$$

$$DIB_k = \frac{(LUB_{kt} - LUB_{kt-1})/LUB_{kt-1}}{(GDP_{kt} - GDP_{kt-1})/GDP_{kt-1}} = \frac{\Delta LUB}{\Delta GDP} \quad (3)$$

where DIE_k and DIB_k represent the decoupling index between ERI and GDP, and between the area of CL and GDP, respectively, in the kth grid; ERI_{kt} and ERI_{kt-1} represent the ERI values in the kth grid for years t-th and $t-1$; LUB_{kt} and LUB_{kt-1} represent the areas of CL in the kth grid for the same years; GDP_{kt} and GDP_{kt-1} represent GDP values in the kth grid for the same years; ΔERI represents the growth rate of ERI; ΔLUB represents the growth rate of CL area; and ΔGDP represents the EG rate. The decoupling results of the model were divided into eight categories based on cut-off points of 0, 0.8, and 1.2 [50]. The specific classification types and their meanings are listed in Table 3.

Table 3. Eight Classification Types and Meanings for the Decoupling Model.

Decoupling State		$\Delta ERI/\Delta LUB$ [1]	ΔGDP	Decoupling Index	Meaning
Decoupling	Strong decoupling	< 0	≥ 0	$DIE/DIB < 0$	The most ideal state is when EG occurs along with a decrease in *ERI* or the area of CL.
	Weak decoupling	> 0	≥ 0	$0 \leq IE/DIB < 0.8$	A relatively ideal state is when EG occurs, but *ERI* or the area of CL increase slowly.
	recessive decoupling	< 0	< 0	$IE/DIB > 1.2$	A better state is when economic recession occurs, along with a significant decrease in *ERI* or the area of CL.
Negative decoupling	Strong negative decoupling	≥ 0	< 0	$IE/DIB < 0$	The least ideal state is when economic recession occurs, and *ERI* or the area of CL increases.
	Weak negative decoupling	< 0	< 0	$0 < IE/DIB < 0.8$	A very unfavorable state is when economic recession occurs, but *ERI* or the area of CL decreases slowly.
	Expansive negative decoupling	≥ 0	≥ 0	$IE/DIB > 1.2$	A relatively unfavorable state is when EG is slow, but *ERI* or the area of CL increases significantly.
Connect	Growth connection	≥ 0	≥ 0	$0.8 < IE/DIB < 1.2$	It is also possible that EG occurs simultaneously with the growth of *ERI* or the area of CL.
	Declining connection	< 0	< 0	$0.8 < IE/DIB < 1.2$	Economic recession can occur simultaneously with the decrease in *ERI* or the area of CL.

[1] The "/" symbol in this table is an or, and in other formulas it is a division sign.

2.3.4. Spatial Autocorrelation Analysis

The spatial autocorrelation analysis assessed the correlation between a spatial variable and its location [51]. To better reveal the spatial distribution and patterns of the study subjects, global and local Moran's indices (Moran's I) were used to reflect spatial heterogeneity.

Global *Moran's I* can be expressed as follows:

$$Moran's\ I = \frac{n\sum_i \sum_j w_{ij}(S_i - \bar{s})(S_j - \bar{s})}{\left(\sum_i \sum_j w_{ij}\right)\sum_j (S_j - \bar{s})(S_j - \bar{s})} \quad (4)$$

where s_i and s_j are the spatial cells of s in neighboring pairs; w_{ij} is the null weight matrix; and $\bar{s}$ is the mean value of an attribute.

Local Moran's I can be expressed as follows:

$$LISA_i = \frac{(S_i - \bar{s})}{\sum_i (S_i - \bar{s})(S_i - \bar{s})/n}\sum_j w_{ij}(w_j - \bar{s}) \quad (5)$$

LISA is essentially *Moran's I* for each region *i*, reflecting the correlation of geographical phenomena in a region *i* with the surrounding region, thus identifying "hot spots" and "cold spots".

3. Results

3.1. Spatial and Temporal Evolution of Landscape Ecology Risk

In this study, the ERI assessment model evaluated the ERI in the BTH region every five years since 1995. The results were categorized into five risk levels using the natural break method (Figure 3), indicating the extent of surface cover change. Higher ERI values signified areas undergoing land use changes, whereas lower values represented stable regions. The ERI in the BTH region exhibited distinct spatial and temporal evolution. High-risk areas were mainly concentrated in mountainous and agro-forestry mixed zones

because of frequent conversions between forest, grassland, and cultivated land. Conversely, the risk in plains areas was closely related to urban expansion and CL growth.

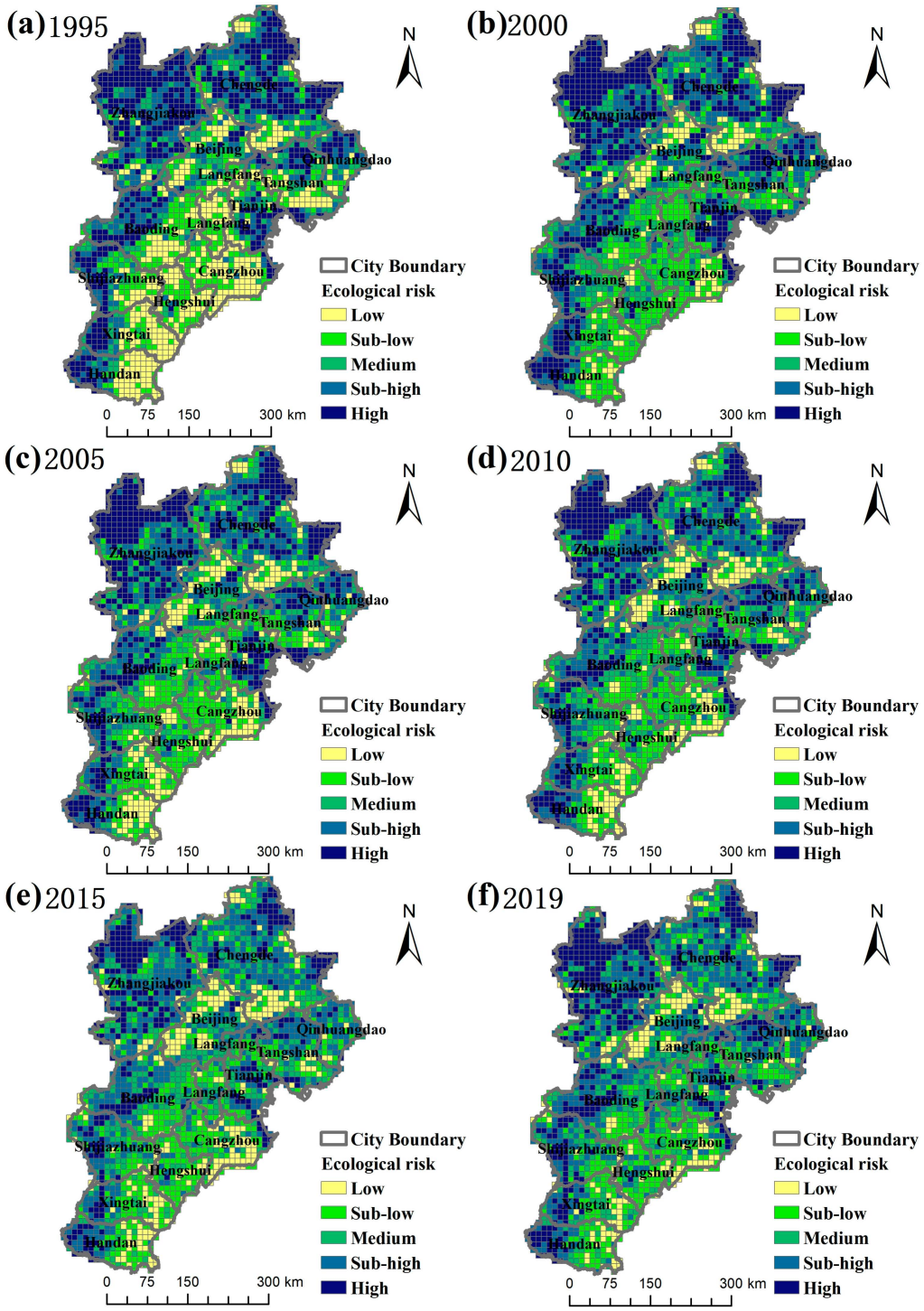


Figure 3. Spatial Distribution of ERI from 1995 to 2019 ((**a**) Results for 1995, (**b**) Results for 2000, (**c**) Results for 2005, (**d**) Results for 2010, (**e**) Results for 2015, (**f**) Results for 2019).

Given that the Zhangjiakou region has had a persistently high risk for a large area over the past 30 years, it has become a typical case study for exploring the interaction and impact between human activities and the natural environment. Therefore, it is particularly important to analyze the city's ecological shifts and the driving forces behind them. The analysis showed that the occurrence of this situation in the region was mainly attributed to

developed agriculture, with the rapid transformation of grassland, the main land type, into cultivated land. Cultivated land accounts for approximately 68% of the area, constantly disrupting the surface ecosystem. Statistical grid data analysis revealed that the grassland area in Zhangjiakou was 15,399.49 km^2 in 1990, 14,900.94 km^2 in 1995, 15,740.88 km^2 in 2000, 17,602.16 km^2 in 2015, and 16,041.59 km^2 in 2019.

It is evident that the year 2000 was the turning point. Since the implementation of the Grain for Green Policy in 2000, Zhangjiakou has had the annual task of returning 6666 ha^2 of farmland to grassland, leading to an increase in grassland area. By 2015, grassland areas had peaked [52]. Concurrently, the high-risk areas in Zhangjiakou diminished significantly in 2015. However, as the animal husbandry economy increasingly developed and extreme weather events became more frequent, grasslands began to degrade. In 2019, the grassland area of Zhangjiakou decreased, accompanied by an increase in the number of high-risk zones.

The plain south of the BTH region was mainly at low risk in 1995; however, its risk level gradually increased over time. The ecological risk in this region increased significantly in 2000. According to the analysis in Table 4, this was mainly related to rapid urban expansion and the conversion of a large amount of cultivated land into CL. Although the subsequent CL growth remained high, its spatial distribution became more dispersed and did not concentrate around urban areas, as in 2000. Consequently, this has not led to a widespread increase in ecological risk.

Table 4. Statistics of ERI and CL Area.

Index	1995	2000	2005	2010	2015	2019
Minimum value	0.0036	0.0033	0.0031	0.0030	0.0030	0.0035
Maximum value	0.0793	0.0807	0.0766	0.0746	0.0710	0.0712
Mean value	0.0362	0.0391	0.0374	0.0372	0.0357	0.0372
Standard deviation	0.0145	0.0131	0.0130	0.0123	0.0117	0.0112
Construction land area (km^2)	19,347.19	21,667.18	23,727.92	26,776.15	30,208.87	31,848.78

3.2. Analysis of Hotspots

When judging the decoupling relationship, the correlation between the growth rates of ERI, CL, and EG was crucial. Therefore, before conducting the decoupling analysis, we analyzed the spatial clustering and differential characteristics of these three growth rates to gain a deeper understanding of the changing mechanism of the decoupling relationship between ERI/CAG and EG. Using the univariate local Moran's I in GeoDa's spatial analysis function(version 1.22), we conducted hotspot analysis, and the results are depicted in Figures 4–6.

The analysis of the results revealed that the most significant change in the growth rate of the ERI occurred from 1995 to 2000. During this stage, significant low-low clustering was observed in the northern (mainly concentrated in Zhangjiakou and Chengde) and western (composed of the western regions of Beijing, Baoding, Shijiazhuang, Xingtai, Handan, and other areas) marginal areas of BTH. During this period, there was marked high-high clustering in the southeastern plains. This indicates that the growth of the ERI was relatively slow in the northern and western marginal areas, and there was an increasing emphasis on protecting mountainous areas. In the southeastern plains, there was rapid growth, with hotspots mainly distributed in densely populated areas such as Langfang, Tianjin, Cangzhou, Hengshui, Xingtai, and Baoding forming a whole [13]. Since 2000, the ERI growth rate in the southeast has no longer exhibited large-scale high-high or low-low clustering, but has gradually transformed into more dispersed and fragmented small-scale clustering. From 2015 to 2019, a distinct high-high clustering region was formed in Zhangjiakou. These changes indicate that before 2000, the ERI growth rate in the BTH region showed a northwest-low and southeast-high clustering pattern. After 2000, the high-high clustering areas were mainly concentrated in the southeastern region, with a trend of mutual conversion between high-high and low-low clustering.

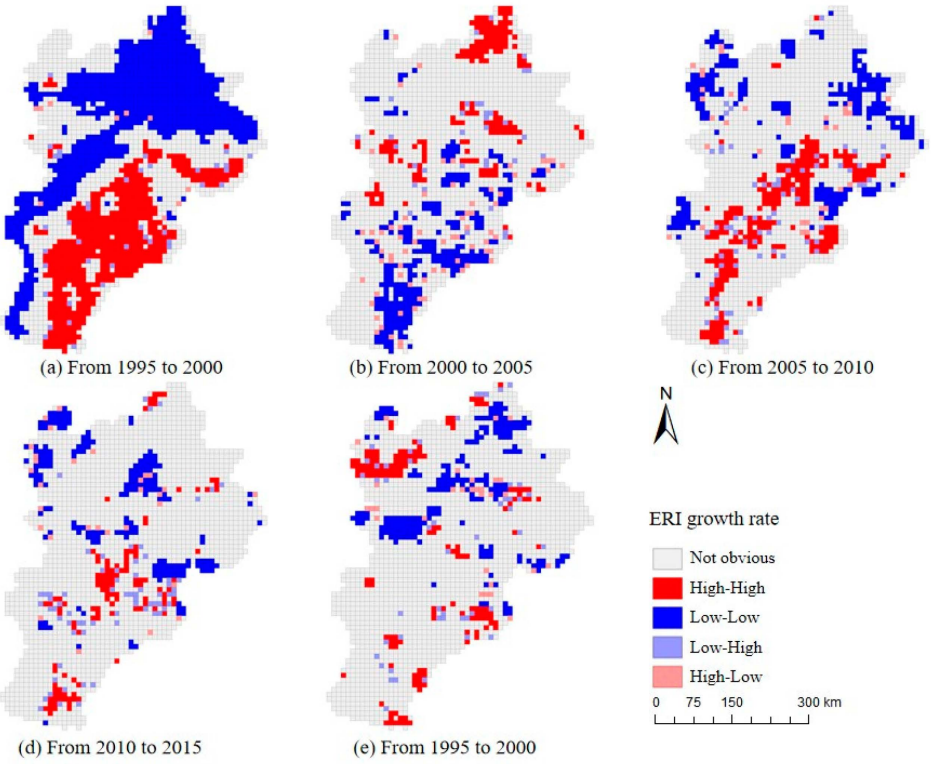


Figure 4. Hotspot Analysis of Growth Rate of ERI from 1995 to 2019 ((**a**) Results of growth rate of ERI hotspot analysis from 1995 to 2000, (**b**) Results from 2000 to 2005, (**c**) Results from 2005 to 2010, (**d**) Results from 2010 to 2015, (**e**) Results from 2015 to 2019).

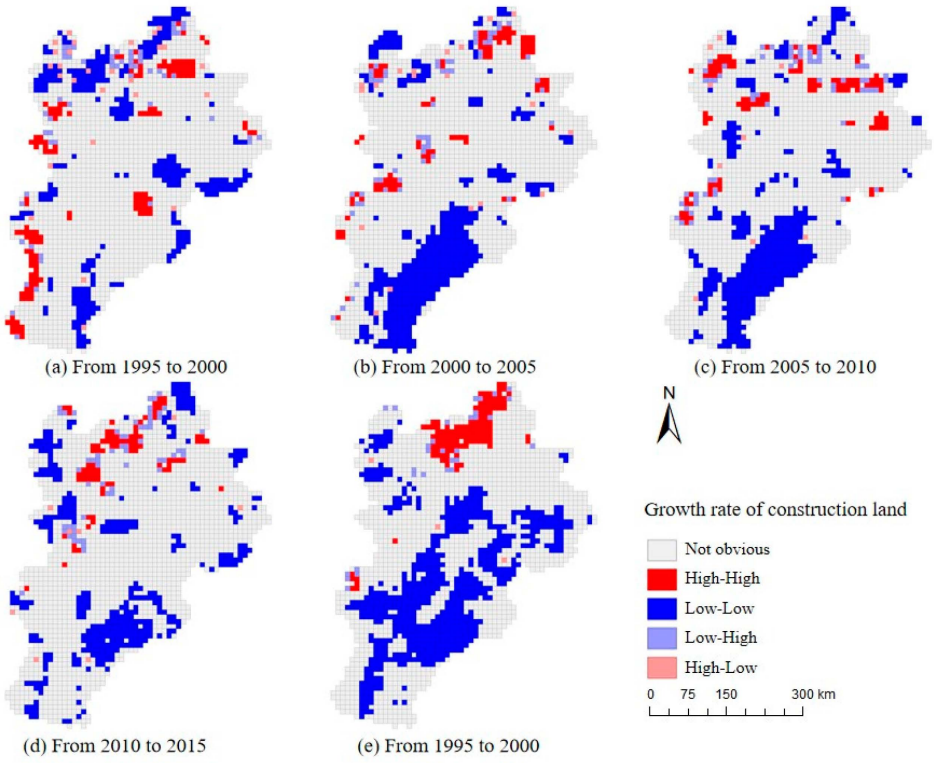


Figure 5. Hotspot Analysis of Growth Rate of CL Area from 1995 to 2019. ((**a**) Results of growth rate of CL area hotspot analysis from 1995 to 2000, (**b**) Results from 2000 to 2005, (**c**) Results from 2005 to 2010, (**d**) Results from 2010 to 2015, (**e**) Results from 2015 to 2019).

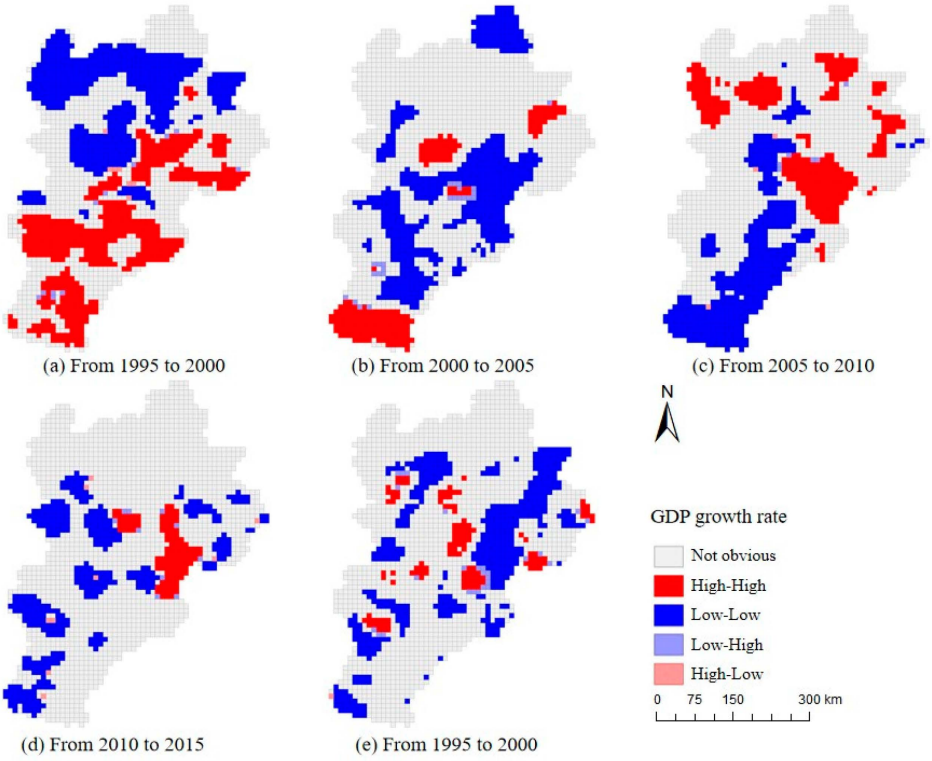


Figure 6. Hotspot Analysis of GDP Growth Rate from 1995 to 2019. ((**a**) Results of growth rate of GDP hotspot analysis from 1995 to 2000, (**b**) Results from 2000 to 2005, (**c**) Results from 2005 to 2010, (**d**) Results from 2010 to 2015, (**e**) Results from 2015 to 2019).

Hotspot analysis of the CL use growth rate revealed a general pattern of large-scale low-low clustering in the southeast and small-scale high-high clustering in the northwest. Despite the significant increase in the total CL area in the BTH region (Table 4), the growth rate of the CL area was relatively low because of the fine grid division at the grid scale, exhibiting a phenomenon of low-value clustering of growth rates. Therefore, before 2000, the growth in CL use in the southeast was minimal, with a small area of low-low clustering mainly concentrated in Beijing, Tianjin, and Handan. After 2000, although CL use increased substantially in the southeast, the scattered distribution had a relatively low growth rate at the grid scale.

From 1995 to 2000, cities in the southern BTH region, including Handan, Xingtai, Shijiazhuang, Hengshui, Beijing, and Tianjin, exhibited widespread high-high clustering in GDP growth. Zhangjiakou, Chengde, and Baoding exhibited larger areas of low-low clustering. However, after 2005–2010, the GDP growth in Handan gradually slowed, exhibiting low-low clustering, along with Xingtai, Hengshui, and Cangzhou. After 2015, GDP growth declined across the BTH region, with extensive low-low clustering, whereas high-high clustering decreased and became more scattered. Tianjin and Beijing showed relatively rapid growth, whereas other regions had lower growth rates. The GDP hotspot analysis trends in this study aligned with those of Tang et al. [53], thus verifying the validity of this study.

3.3. Decoupling Results

3.3.1. Decoupling Results of ERI Changes

The BTH region, a pivotal economic driver in China, has experienced rapid urban construction and EG, accompanied by the expansion of CL, leading to an increase in ERI. This study focuses on the dynamic relationship between risk change, CL growth, and EG. According to the decoupling results (Figure 7), the decoupling relationship between the ERI and EG in the BTH region exhibited complex changes across different periods

and spatial scales. These fluctuations were shaped by multifaceted factors, including economic development, environmental protection policies, and regional cooperation, and underscored the region's ongoing pursuit of an economic-ecological balance.

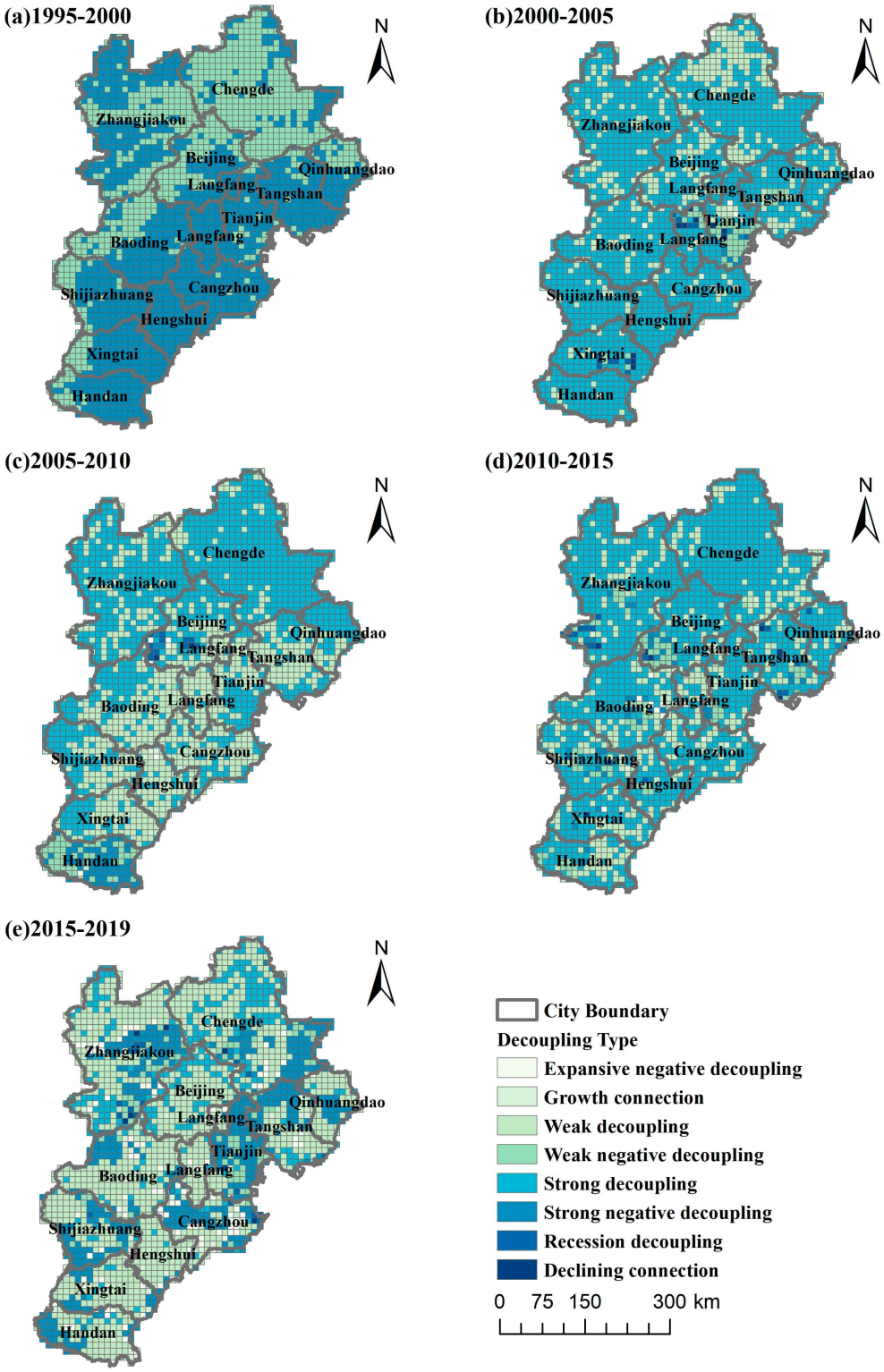


Figure 7. Spatial Distribution of Decoupling between ERI and EG from 1995 to 2019. ((**a**) Results of ERI and EG decoupling from 1995 to 2000, (**b**) Results from 2000 to 2005, (**c**) Results from 2005 to 2010, (**d**) Results from 2010 to 2015, (**e**) Results from 2015 to 2019).

Specifically, during 1995–2000, the southeastern part of the BTH region exhibited strong negative decoupling, indicating that the ecological risk increased against the backdrop of an economic recession, which was a highly undesirable situation. The northwestern region primarily demonstrated weak negative decoupling with an economic recession accompanied by a gradual decrease in ecological risk. A particular event during this period was the cancelation of the North China Economic and Technological Cooperation Conference and the low tide in the Beijing Economic Cooperation Zone. These factors have led to blind construction in various regions of the BTH area, further triggering economic recession and increasing ecological risk.

During 2000–2005, various measures such as the "Two Rings Opening-Up Strategy" enabled rapid EG in the BTH region, while environmental protection measures were also effectively implemented. During this period, the decoupling relationship between the ERI and EG primarily featured strong and weak decoupling, indicating a relatively ideal development across most BTH regions. From 2005 to 2010, most regions were dominated by strong or weak decoupling. The relationship between economic development and ERI in these regions is relatively ideal. Affected by economic development, Handan was in a state of economic recession during this period, dominated by strong and weak negative decoupling.

During 2010–2015, most regions exhibited either strong or weak decoupling, with only a few areas, such as the Fangshan District in Beijing, displaying a mixed state of strong and weak negative decoupling; the ERI and economic development were balanced and ideal. From 2015 to 2019, the regions experiencing strong negative decoupling expanded, with regions in Zhangjiakou, Chengde, Tangshan, Tianjin, Cangzhou, and Shijiazhuang shifting from strong/weak to strong negative decoupling. Beijing, Baoding, Langfang, Hengshui, Xingtai, and other regions were in a mixed state of strong and weak decoupling or were mainly characterized by weak decoupling, indicating relatively ideal development conditions.

3.3.2. Decoupling Results of Construction Area Changes

Analysis of the decoupling results between the expansion of the CL and EG in the BTH region (Figure 8) revealed distinct period-specific characteristics in their decoupling relationship. It presented a pattern of weak decoupling in most periods, with local aggregation/replacement of other decoupling types. The study showed a clear, strong negative decoupling from 1995 to 2000. During this stage, influenced by various unfavorable factors (such as the cancelation of the North China Economic and Technological Cooperation Conference), the economy was in recession, and the growth of CL exhibited a state of blind expansion.

This has resulted in an unbalanced relationship between CL expansion and economic development in the entire BTH region. This did not bode well for long-term regional development. From 2000 to 2005, the economic environment of the BTH region improved significantly. Except for Tianjin, which exhibited strong negative decoupling, the other areas exhibited weak decoupling. During this period, the EG was accompanied by a slow increase in the CL area, greatly improving the coupling relationship between CL expansion and EG in the BTH region.

From 2005 to 2010, Fangshan District in Beijing shifted from weak decoupling to a mixed state of strong and weak negative decoupling. Owing to the limitations of local industrial types, Handan experienced an economic recession, and the decoupling relationship between the expansion of the CL and EG shifted to a weak negative decoupling. From 2010 to 2015, a notable coupling relationship occurred between CL expansion and EG in the BTH region. Although weak decoupling remained dominant, growth-negative decoupling and strong negative decoupling gradually expanded in some small local areas.

From 2015 to 2019, the decoupling relationship between CL and EG in the BTH region exhibited a substantial contraction in the area of weak decoupling, accompanied by a rapid expansion of strong negative decoupling and growth negative decoupling. This implies that during periods of economic slowdown or recession, the expansion of CL accelerated.

This situation neither promoted regional economic development nor resulted in a waste of land resources. With reference to similar studies, it is advisable to adopt planning regulations and other means to mitigate the rate of CL expansion, foster locally distinctive industries, and promote regional EG [19].

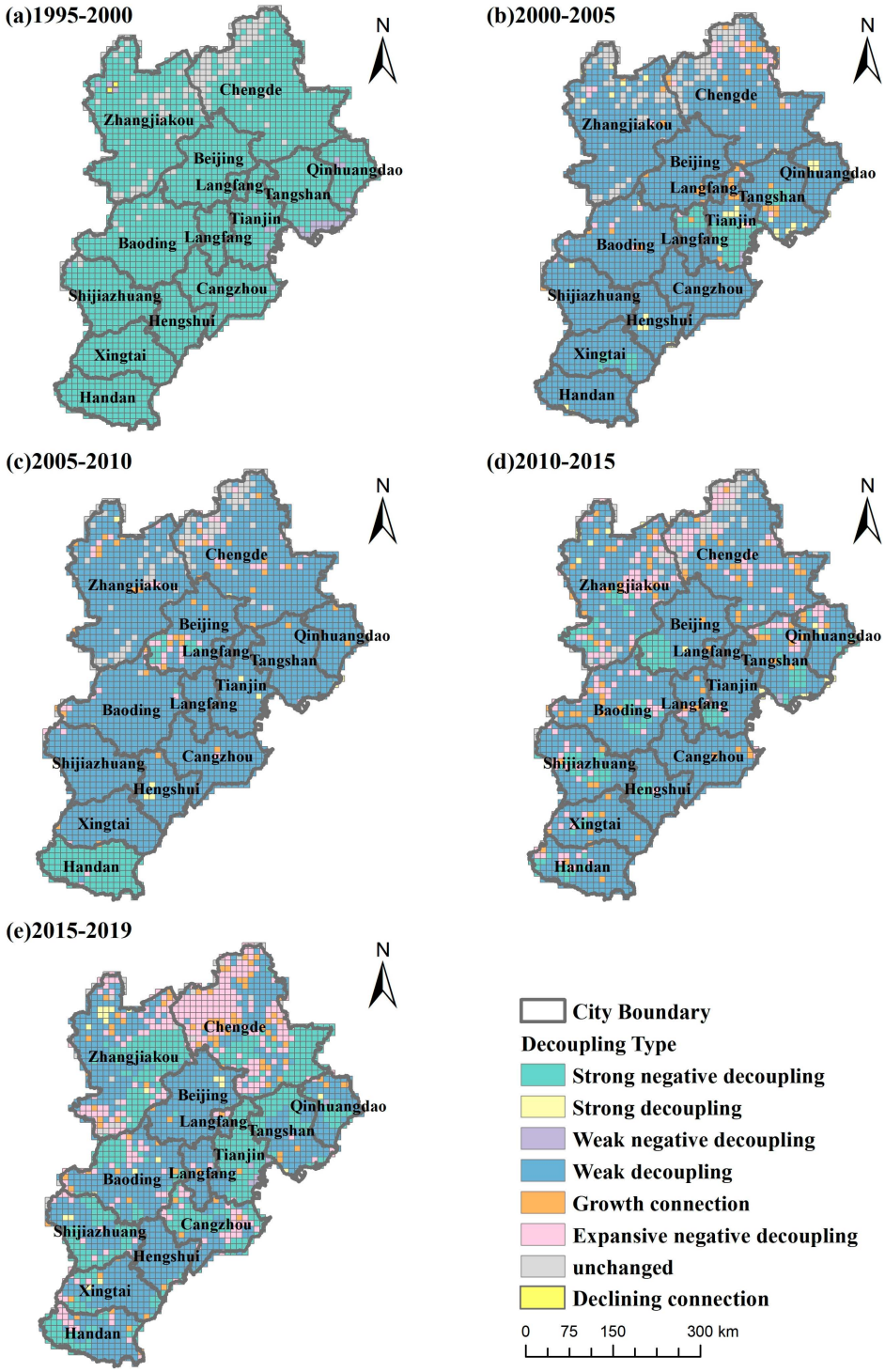


Figure 8. Spatial distribution of decoupling between changes in CL area and EG from 1995 to 2019. ((**a**) Results of CL area and EG decoupling from 1995 to 2000, (**b**) Results from 2000 to 2005, (**c**) Results from 2005 to 2010, (**d**) Results from 2010 to 2015, (**e**) Results from 2015 to 2019). * unchanged refers to no CL /no change in CL area within the grid.

3.4. Spatial Heterogeneity Analysis

This study employed the spatial analysis module of ArcGIS 10.3 to investigate the spatial heterogeneity of the decoupling relationship between ERI, CL expansion, and EG in the BTH region (Table 5). By calculating Moran's I, we found that the decoupling relationship of the ERI was randomly distributed. Therefore, we do not discuss this further.

Table 5. Decoupling statistical variables of changes in CL area.

Statistical Variables	1995–2000	2000–2005	2005–2010	2010–2015	2010–2019
Moran's I	0.0060	0.1155	0.1027	0.1280	0.1310
z	15.19	11.87	7.59	9.74	8.95
p	0	0	0	0	0

The spatial correlation of the decoupling relationship between the CL expansion and EG passed the significance test for *p*-values in all periods. Overall, spatial autocorrelation gradually increased. Although Moran's I values in different periods fluctuated around 0.1, indicating a certain degree of spatial aggregation in the decoupling relationship between CL and EG, the overall trend was insignificant. The decoupling relationship between CL expansion and EG in the BTH region evolved in two stages: before 2005, the spatial autocorrelation of the decoupling relationship gradually increased, slightly decreased from 2005 to 2010, and then increased again after 2005. Combined with previous research, we can infer that the CL expansion around 2000 revolved around urban areas, exhibiting high spatial aggregation. Subsequently, CL expansion shifted to rural areas, resulting in a more dispersed distribution. The enhanced spatial autocorrelation in both stages may be closely related to changes in the pattern of CL expansion.

4. Discussion

4.1. Consideration of Scale

In selecting the analysis scale for this study, we primarily referred to Xu et al. (2021), who discussed in detail the relationship between landscape structural changes and the thermal environment at different scales within the BTH region, pointing out that the analysis effect was optimal at the 10 km scale [38]. Combined with the research of Lin et al. (2021), this scale helped accurately assess landscape ecological risks and ensured computational accuracy while controlling the workload [54]. Therefore, this study focused on relevant issues at the 10 km scale and carried out an in-depth discussion.

During the comparative analysis of the raster and statistical yearbook data based on administrative regions, we found certain differences between the two. Particularly in the BTH region, some indicators that showed significant changes at the administrative scale (such as the growth rate of CL) exhibited relatively limited changes at the grid scale. This also resulted in a widespread low-low clustering phenomenon of CL growth rates in the southeastern plain areas during hot spot analysis. Through further analysis and reference to relevant studies [55], it was found that the southeastern plain area was dominated by cultivated land, which was also the main source of CL growth. Before 2000, this growth revolved around urban areas, whereas after 2000, it shifted to a more dispersed rural expansion. Although the total amount of the dispersed CL growth was large, it was relatively small at the grid scale. To address this challenge, future research should optimize the grid scale and comprehensively consider the performance characteristics of the indicators at different scales.

4.2. Considerations on Indicator Selection

After the reform and opening up, China's economy achieved rapid growth; however, this growth was often accompanied by excessive consumption of environmental resources. This extensive development model leads to a tremendous waste of resources and causes serious environmental problems, such as disorderly urban expansion, air pollution, and

unregulated discharge of industrial wastewater [56]. More importantly, this development model carries a long-term sustainability risk. Excessive extraction and consumption of resources have led to the rapid depletion of natural resources, which has severely constrained further economic development. As key resources became scarce, production costs surged, and the stability and security of industrial chains were jeopardized. Environmental pollution and ecological disruption pose long-term risks to public health. In response to these challenges, the Chinese government has gradually recognized the importance of sustainable development and implemented a series of ecological restoration and protection measures. For example, the Grain for Green Project launched in 2000 aims to maintain ecosystem stability by restoring forest and grassland resources. Subsequently, President Xi Jinping proposed the important assertion of "Lucid waters and lush mountains are invaluable assets" in 2005 [57]. By 2021, President Xi Jinping further emphasized the strategic task of building a beautiful China at the National Conference on Ecological and Environmental Protection, first emphasizing the protection of the ecological environment. There have been varying degrees of improvements across counties and regions. Chengdu has gradually adjusted its industrial structure and layout, focusing on economic development and reducing land resource waste [16].

Against this backdrop, China is undergoing a transition from a traditional and extensive economy to an intensive one. During this transition, significant changes have occurred in China's surface landscape ecology owing to various factors such as economic development and policy adjustments. Therefore, a thorough exploration of the relationship between landscape ecology and EG over a long period is of great significance for guiding the coordinated progress of economic development and ecological protection. This study focuses on the impact of EG on the landscape ecological environment and constructs a decoupling model on a grid scale to quantify the correlation between indicators. Given the extensiveness and complexity of landscape ecology, this study adopted the ERI as a measure of changes in landscape ecology due to external interference [58]. Considering that CL was the main carrier of EG, its growth was closely linked to economic development and land type changes [59]. Therefore, this study selected CL growth as the driving force of landscape ecological changes and the landscape risk index as the result of changes in the landscape ecological environment. By exploring the coupling relationship between the growth of CL, landscape risk index, and EG, this study aimed to provide scientific evidence for achieving sustainable development of the economy and environment.

4.3. Comparison with Similar Studies

The novelty of this study lies in the construction of a decoupling model at the grid scale to quantify the relationship between the ERI, CL growth, and EG. This scale selection was more detailed and accurate than traditional administrative unit scales (provincial, prefectural, and county levels). For example, Yan and Chen (2022) examined the decoupling status of the construction industry's economic development and carbon dioxide emissions at the provincial scale [60]; Xia et al. (2020) studied the impact of socioeconomic factors on industrial air pollutant emissions at the prefecture-level city scale [61]; and Zhang et al. (2022) analyzed the decoupling relationship between carbon emissions and EG at the county level and studied the spatiotemporal evolution characteristics and spatial aggregation patterns of that decoupling relationship [62].

Despite the increasingly detailed results exhibited by research conducted at administrative unit scales, ranging from the provincial to prefecture level and further down to the county level, there are still certain limitations when compared to the grid scale. At the grid scale, we captured subtle changes in the decoupling relationships between variables with greater precision. For instance, in the Zhangjiakou region, the grid scale enabled us to identify the transition of the decoupling relationship from strong negative decoupling to growth negative decoupling in small-scale areas. Such changes might have been overlooked at the administrative unit scale because the data for the entire administrative unit were simplified into a single value, making it challenging to accurately determine the specific reasons for

changes in the decoupling relationship. Similarly, even at the district or county level, such as Fangshan District in Beijing, the grid-scale could reveal the existence of multiple decoupling relationships within the region, which is difficult to achieve at the administrative unit scale. Of course, there were also shortcomings at the grid scale, such as difficulties in data acquisition, difficulty in ensuring data quality, and high workload, which must be overcome.

4.4. Suggestions and Future Work

This research initially explored the decoupling relationship between ERI, growth of the CL area, and EG, and conducted a study on the spatial distribution patterns over a long time series. When EG ceased to rely on the expansion of CL, and the reduction in CL area controlled the disturbance to ecosystems, virtuous social development could be achieved, marking the attainment of a decoupling state. The realization of decoupling facilitated green transformation and sustainable development of industries, harmonizing economic construction with ecological protection.

To further strengthen the policy discussion and provide actionable suggestions, the following specific planning measures should be considered: (1) Ecosystem-based land-use planning: land-use planning should prioritize the protection and restoration of critical ecosystems. By identifying landscape ecological risk areas to protect wetlands, forests, and biodiversity, the impact of urban expansion on natural habitats can be minimized. In addition, integrating green infrastructure such as urban parks and green roofs can enhance urban resilience and improve ecological connectivity. (2) Compact and efficient urban development: encouraging compact and efficient urban development patterns can reduce the need for additional CL. This includes promoting high-density mixed-use developments that minimize the urban footprint while supporting vibrant and sustainable communities. By optimizing land use, population growth and economic activities can be accommodated without compromising ecological integrity. (3) Community engagement and education: engaging communities in land-use planning processes and educating them on the importance of ecological conservation can foster a sense of ownership and responsibility. By involving stakeholders at all levels, we can ensure that the planning measures are effective, acceptable, and sustainable in the long term.

However, some issues remain in the research process, such as the selection of the grid scale, which needs to be optimized in future studies. Future research can further elucidate the reasons for the changes in decoupling patterns in the BTH region. By selecting the potential influencing factors for research, we can gain a more comprehensive understanding of the dynamic evolution of decoupling relationships. In addition, combining a decoupling relationship with policy planning and industrial forms is a worthwhile research direction. By exploring the impact of policy planning and industrial forms on decoupling distribution patterns, we provide scientific evidence for policymakers to guide them in formulating more reasonable and sustainable policies and industrial development strategies. Meanwhile, through scenario simulation studies, we can predict and adjust policy planning and industrial forms when decoupling relationships change, optimize the decoupling types, and achieve sustainable and healthy EG. Overall, future research should focus on addressing the issues in current studies, analyzing the causes of decoupling relationships, exploring the impact of policy planning and industrial forms on decoupling distribution patterns, and proposing strategies and suggestions for optimizing decoupling types through scenario simulation studies. These studies contribute to the promotion of sustainable development in the BTH region and provide scientific evidence for relevant policy formulations.

5. Conclusions

This study conducted a thorough analysis of the causes of landscape ecological changes, considering CL growth as a key factor driving changes in surface cover. By utilizing ERI as a quantifiable indicator, we constructed a decoupling model at the grid scale to explore the coupling relationships, change mechanisms, and spatiotemporal distribution patterns of ERI, CL growth, and EG over a long time series. Key findings include:

(1) The ERI reached its highest value in 2000, accompanied by significant spatial distribution changes. Notably, the southeastern plain region transitioned from low to medium or high ecological risk. Hotspot analysis revealed that CL and GDP growth rate hotspots were more consistent than the ERI hotspots. Over time, the ERI hotspots shifted southward with a scattered distribution, whereas the CL growth hotspots expanded northward. GDP growth hotspots initially shifted from south to north, but eventually presented a mixed pattern.

(2) The decoupling relationship between ERI and EG transitioned from unfavorable (strong and weak negative decoupling) to ideal (strong and weak decoupling), and then returned to unfavorable (weak decoupling and strong negative decoupling). Similarly, the CL area and EG decoupling evolved from strong negative to weak decoupling, ultimately forming a decoupling state in which multiple decoupling types coexisted.

(3) The decoupling relationship between ERI, CAG, and EG exhibited dynamic and complex changes influenced by government planning, environmental policies, and regional collaboration. To achieve balanced, healthy, and sustainable regional development, relevant departments should adopt reasonable planning strategies, adjust CL-EG relationships, strengthen ecological protection, and seek a balance between economic and ecological interests.

Author Contributions: Conceptualization, X.W., M.Z., D.L. and X.Z. (Xinqi Zheng); Data curation, X.W. and X.Z. (Xiaoyuan Zhang); Formal analysis, X.W.; Funding acquisition, M.Z. and X.Z. (Xinqi Zheng); Methodology, X.W., M.Z., X.Z. (Xinqi Zheng) and Y.M.; Supervision, P.W., F.X. and T.R.; Visualization, X.W.; Writing—original draft, X.W.; Writing—review and editing, M.Z., D.L., P.W., X.Z. (Xinqi Zheng), Y.M., F.X., X.Z. (Xiaoyuan Zhang) and T.R. All authors have read and agreed to the published version of the manuscript.

Funding: This work was supported by the National Natural Science Foundation of China (72033005); Science and Technology Project of China Land Survey and Planning Institute, Ministry of Natural Resources (20221811134); "Deep-time Digital Earth" Science and Technology Leading Talents Team Funds for the Central Universities for the Frontiers Science Center for Deep-time Digital Earth, China University of Geosciences (Beijing) (Fundamental Research Funds for the Central Universities; grant number: 2652023001); the Third Xinjiang Scientific Expedition of the Key Research and Development Program by Ministry of Science and Technology of the People's Republic of China (No. 2022xjkk1104); the Fundamental Research Funds for the Central Universities under Grant (No. 2652023060). This research was supported by the National Natural Science Foundation of China (No. 42401520). National Natural Science Foundation of China (No. 42201471).

Data Availability Statement: Data available on request due to restrictions (e.g., privacy, legal or ethical reasons). The data presented in this study are available on request from the corresponding author due to (Graduation requires).

Conflicts of Interest: The authors declare that they have no known competing financial interests or personal relationships that could have appeared to influence the work reported in this paper.

References

1. Aburas, M.M.; Abdullah, S.H.O.; Ramli, M.F.; Asha'ari, Z.H. Land Suitability Analysis of Urban Growth in Seremban Malaysia, Using GIS Based Analytical Hierarchy Process. *Procedia Eng.* **2017**, *198*, 1128–1136. [CrossRef]
2. Yu, J.; Zhou, K.; Yang, S. Land use efficiency and influencing factors of urban agglomerations in China. *Land Use Policy* **2019**, *88*, 104143. [CrossRef]
3. Liang, L.; Chen, M.; Lu, D. Revisiting the Relationship Between Urbanization and Economic Development in China Since the Reform and Opening-up. *Chin. Geogr. Sci.* **2022**, *32*, 1–15. [CrossRef]
4. Liu, C.; Cheng, L.; Li, J.; Lu, X.; Xu, Y.; Yang, Q. Trade-offs analysis of land use functions in a hilly-mountainous city of northwest Hubei Province: The interactive effects of urbanization and ecological construction. *Habitat Int.* **2023**, *131*, 102705. [CrossRef]
5. Qu, Y.; Zhan, L.; Wei, C.; Zhang, Q.; Wang, J. Interactive transition of cultivated land and construction land during china's urbanization: A coordinated analytical framework of explicit and implicit forms. *Land Use Policy* **2024**, *138*, 107049. [CrossRef]
6. Li, Y.; Zhen, W.N.; Luo, B.B.; Shi, D.H.; Li, Z.H. Analyzing Spatial-Temporal Characteristics and Influencing Mechanisms of Landscape Changes in the Context of Comprehensive Urban Expansion Using Remote Sensing. *Remote Sens.* **2024**, *16*, 2113. [CrossRef]
7. Feng, F.; Wang, L.L.; Hou, W.X.; Yang, R.; Zhang, S.W.; Zhao, W.J. Analyzing the dynamic changes and causes of greenspace landscape patterns in Beijing plains. *Ecol. Indic.* **2024**, *158*, 111556. [CrossRef]

8. Wang, X.B.; Xu, Z.; Huang, J.; Zhang, Z.F. Spatiotemporal Evolution and Factors Influencing Regional Ecological Land in a Multidimensional Perspective: A Case Study of the Beijing-Tianjin-Hebei Region. *Remote Sens.* **2024**, *16*, 1714. [CrossRef]
9. Chang, S.; Wei, Y.Q.; Dai, Z.Z.; Xu, W.; Wang, X.; Duan, J.J.; Zou, L.; Zhao, G.R.; Ren, X.Y.; Feng, Y.Z. Landscape ecological risk assessment and its driving factors in the Weihe River basin, China. *J. Arid Land* **2024**, *16*, 603–614. [CrossRef]
10. Yang, S.Q.; Jin, Z. Impact of road network expansion on landscape ecological risk and soil erosion sensitivity on the Luochuan Tableland of the Chinese Loess Plateau. *Reg. Environ. Chang.* **2024**, *24*, 37. [CrossRef]
11. Zhang, X.; Du, H.; Wang, Y.; Chen, Y.; Ma, L.; Dong, T. Watershed landscape ecological risk assessment and landscape pattern optimization: Take Fujiang River Basin as an example. *Hum. Ecol. Risk Assess. Int. J.* **2021**, *27*, 2254–2276. [CrossRef]
12. Shi, Y.; Gao, H.; Tan, S.; Qin, H.; Tian, Z.; Meng, J.; Zheng, X. Pattern change and ecological risk analysis of Shilin World Geopark landscape. *Front. Ecol. Evol.* **2024**, *12*, 1341969. [CrossRef]
13. Cheng, X.; Zhang, Y.; Yang, G.; Nie, W.; Wang, Y.; Wang, J.; Xu, B. Landscape ecological risk assessment and influencing factor analysis of basins in suburban areas of large cities—A case study of the Fuchunjiang River Basin, China. *Front. Ecol. Evol.* **2023**, *11*, 1184273. [CrossRef]
14. Zhong, N.; Xia, R.; Zhang, H.; Dou, J.; Chen, Y.; Jia, R.; Yin, Y.; Yan, C. Research on the Decoupling Relationship between Water Resources Utilization and Economic Development in Urban Agglomerations of the Yellow River Basin. *Res. Environ. Sci.* **2024**, *37*, 102–113.
15. Mao, L.; Pei, F.S.; Sun, X.M. Exploring the relationships between human consumption and environmental pressure: A case study of the Yangtze river economic zone in China. *Environ. Sci. Pollut. Res.* **2024**, *31*, 20449–20460. [CrossRef]
16. Xu, M.; Yang, X.; Deng, L.L.; Liao, X.; Niu, Z.S.; Hao, L.N. Decoupling state of urban development and carbon emissions and its driving factors and predictions: A case study of Chengdu metropolitan area. *Ecol. Inform.* **2024**, *82*, 102692. [CrossRef]
17. Ning, Q.; Ouyang, X.; Liu, S. Spatio-Temporal Evolution and Quality Analysis of Construction Land in Urban Agglomerations in Central China. *Front. Ecol. Evol.* **2022**, *10*, 912127. [CrossRef]
18. Xie, Y.; Guo, F.; Zhang, Q.; Jiang, Y.; Chen, W. Decoupling level and driving factors of fossil energy consumption based industrial carbon emissions and economic growth in Jinan. *Environ. Pollut. Control* **2023**, *45*, 1467–1472.
19. Cao, Y.; Xie, Z.; Woodgate, W.; Ma, X.; Cleverly, J.; Pang, Y.; Qin, F.; Huete, A. Ecohydrological decoupling of water storage and vegetation attributed to China's large-scale ecological restoration programs. *J. Hydrol.* **2022**, *615*, 128651. [CrossRef]
20. Wang, K.; Zhu, Y.; Zhang, J. Decoupling economic development from municipal solid waste generation in China's cities: Assessment and prediction based on Tapio method and EKC models. *Waste Manag.* **2021**, *133*, 37–48. [CrossRef]
21. Dony, C.C.; Delmelle, E.M.; Delmelle, E.C. Re-conceptualizing accessibility to parks in multi-modal cities: A Variable-width Floating Catchment Area (VFCA) method. *Landsc. Urban Plan.* **2015**, *143*, 90–99. [CrossRef]
22. Jin, K.; Wu, Y. Boundary-fitted grid in landscape modeling. *Landsc. Ecol.* **1997**, *12*, 19–26. [CrossRef]
23. Wang, X.; Sun, Y.; Liu, Q.; Zhang, L. Construction and Optimization of Ecological Network Based on Landscape Ecological Risk Assessment: A Case Study in Jinan. *Land* **2023**, *12*, 743. [CrossRef]
24. Liao, M.L. Study on the Coupling and Coordination Degree of High-Quality Economic Development and Ecological Environmet in Beijing-Tianjin-Hebei Region. *Appl. Ecol. Environ. Res.* **2019**, *17*, 11069–11083. [CrossRef]
25. Si, Q.; Fan, H.; Dong, W.; Liu, X. Landscape ecological risk assessment and prediction for the Yarkant River Basin, Xinjiang, China. *Arid Zone Res.* **2024**, *41*, 684–696. [CrossRef]
26. Yu, S.; Kang, Y.; Deng, W.; Wang, G.; Wang, H.; Xing, Y. Analysis of Production-Living-Ecological land transformation and landscape ecological risk in the eastern counties of the Taihang Mountain: A case study in Pingshan County. *Chin. J. Eco-Agric.* **2022**, *30*, 1113–1122.
27. Kang, L.; Ma, L.; Liu, Y. Comparing the driving mechanisms of different types of urban construction land expansion: A case study of the Beijing-Tianjin-Hebei region. *J. Geogr. Sci.* **2024**, *34*, 722–744. [CrossRef]
28. Calabrese, J.M.; Fagan, W.F. A comparison test of spatial landscape models for ecological connectivity. *Ecology* **2004**, *85*, 2087–2095.
29. Ding, J.; Wang, D. Ecological Risk Assessment of Rural Landscape of Southern Jiangsu Water Net from the Perspective of "Ecology-Production-Living" SpaceA Case Study of Stone Pool Area. *J. Northwest For. Univ.* **2024**, *39*, 265–273.
30. Li, X.H.; Ai, Z.M.; Yang, Z.; Yao, Y.Y.; Ren, Z.Y.; Hou, M.J.; Li, J.Y.; Cao, X.S.; Li, P.; Zhang, D.H.; et al. Ecological risk assessment and restoration area identification of Pengyang County on the basis of the landscape pattern and function. *Environ. Monit. Assess.* **2023**, *195*, 998. [CrossRef]
31. Li, J.L.; Hu, D.W.; Wang, Y.Z.; Chu, J.L.; Yin, H.W.; Ma, M. Study of identification and simulation of ecological zoning through integration of landscape ecological risk and ecosystem service value. *Sustain. Cities Soc.* **2024**, *107*, 105442. [CrossRef]
32. Qu, M.; Tian, Y.; Liu, B.; Xu, D. Ecological Risk Assessment and Impact Factor Analysis of Ecological Spatial Patterns in Coastal Counties: Taking Dalian Pulandian District as an Example. *Sustainability* **2023**, *15*, 11805. [CrossRef]
33. Lan, J.; Chai, Z.; Tang, X.; Wang, X. Landscape Ecological Risk Assessment and Driving Force Analysis of the Heihe River Basin in the Zhangye Area of China. *Water* **2023**, *15*, 3588. [CrossRef]
34. Tian, H.X.; Wang, T.; Wang, W.; Wu, L.F. Interactive exploration the pyramid coupling and forecasting of the economy, energy and air environment. *Energy Rep.* **2024**, *11*, 4127–4142. [CrossRef]
35. Geng, L.L.; Zhang, Y.Y.; Hui, H.X.; Wang, Y.H.; Xue, Y.J. Response of Urban Ecosystem Carbon Storage to Land Use/Cover Change and Its Vulnerability Based on Major Function-Oriented Zone Planning. *Land* **2023**, *12*, 1563. [CrossRef]
36. Yang, J.; Huang, X. The 30 m annual land cover dataset and its dynamics in China from 1990 to 2019. *Earth Syst. Sci. Data* **2021**, *13*, 3907–3925. [CrossRef]

37. Xu, X. China GDP Spatial Distribution Kilometer Grid Dataset. Resource and Environmental Science Data Registration and Publishing System. 20170. Available online: http://www.resdc.cn/DOI (accessed on 7 June 2023).
38. Xu, M.; Li, J.; Yao, L.; Wu, Q. Analysis of the relationship between surface thermal environment and landscape change in Beijing-Tianjin-Hebei Region under multiple scales. *J. Xi'an Univ. Technol.* **2021**, *37*, 43–52.
39. Yang, K.; Xin, G.; Jiang, H.; Yang, C. Study on Spatiotemporal Changes of Landscape Ecological Risk Based on the Optimal Spatial Scale: A Case Study of Jiangjin District, Chongqing City. *J. Ecol. Rural Environ.* **2021**, *37*, 576–586.
40. Dalloz, M.F.; Crouzeilles, R.; Almeida-Gomes, M.; Papi, B.; Prevedello, J.A. Incorporating landscape ecology metrics into environmental impact assessment in the Brazilian Atlantic Forest. *Perspect. Ecol. Conserv.* **2017**, *15*, 216–220. [CrossRef]
41. Shi, Y.; Feng, C.-C.; Yu, Q.; Han, R.; Guo, L. Contradiction or coordination? The spatiotemporal relationship between landscape ecological risks and urbanization from coupling perspectives in China. *J. Clean. Prod.* **2022**, *363*, 132557. [CrossRef]
42. Zhang, H.; Xu, E. An evaluation of the ecological and environmental security on China's terrestrial ecosystems. *Sci. Rep.* **2017**, *7*, 811. [CrossRef] [PubMed]
43. Cao, Y.; Dong, B.; Xu, H.; Xu, Z.; Wei, Z.; Lu, Z.; Liu, X. Landscape ecological risk assessment of chongming dongtan wetland in shanghai from 1990 to 2020. *Environ. Res. Commun.* **2023**, *5*, 105016. [CrossRef]
44. Jiang, L.; Huang, X.; Wang, F.; Liu, Y.; An, P. Method for evaluating ecological vulnerability under climate change based on remote sensing: A case study. *Ecol. Indic.* **2018**, *85*, 479–486. [CrossRef]
45. Peng, J.; Wang, Y.; Zhang, Y.; Wu, J.; Li, W.; Li, Y. Evaluating the effectiveness of landscape metrics in quantifying spatial patterns. *Ecol. Indic.* **2010**, *10*, 217–223. [CrossRef]
46. Xu, W.; Wang, J.; Zhang, M.; Li, S. Construction of landscape ecological network based on landscape ecological risk assessment in a large-scale opencast coal mine area. *J. Clean. Prod.* **2021**, *286*, 125523. [CrossRef]
47. Zhou, D.; Shi, P.; Wu, X.; Ma, J.; Liang, S. Urbanization spatial expansion and regional landscape ecological risk of Yantai City. *Chin. J. Ecol.* **2014**, *33*, 477–485. [CrossRef]
48. Li, X.; Qu, F.; Guo, Z.; Jiang, D.; Pan, Y.; Chen, X. Decoupling Between Urban and Rural Construction Land. *China Popul. Resour. Environ.* **2008**, *18*, 179–184.
49. Tapio, P. Towards a theory of decoupling: Degrees of decoupling in the EU and the case of road traffic in Finland between 1970 and 2001. *Transp. Policy* **2005**, *12*, 137–151. [CrossRef]
50. Wang, Q.; Wang, S.; Li, R. Determinants of Decoupling Economic Output from Carbon Emission in the Transport Sector: A Comparison Study of Four Municipalities in China. *Int. J. Environ. Res. Public Health* **2019**, *16*, 3729. [CrossRef]
51. Anselin, L. Local Indicators of Spatial Association—LISA. *Geogr. Anal.* **2010**, *27*, 93–115. [CrossRef]
52. Luan, Z.; Tian, X.; Lv, F.; LU, X.; Fan, G.; Li, R. Analysis of Grassland Change Trend and Influencing Factors in Zhangjiakou Plateau from 1980 to 2019 Based on Remote Sensing. *Hebei Univ. Geosci.* **2022**, *45*, 73–79.
53. Tang, X.; Gao, Y.; Liu, Y.; Sun, C. Spatial-temporal Pattern and Causes for GDP per Capita at County Level in Beijing-Tianjin-Hebei Region. *Acta Sci. Nat. Univ. Pekin.* **2017**, *53*, 1089–1098. [CrossRef]
54. Lin, M.; Lin, T.; Jones, L.; Liu, X.; Xing, L.; Sui, J.; Zhang, J.; Ye, H.; Liu, Y.; Zhang, G.; et al. Quantitatively Assessing Ecological Stress of Urbanization on Natural Ecosystems by Using a Landscape-Adjacency Index. *Remote Sens.* **2021**, *13*, 1352. [CrossRef]
55. Lou, P.; Fu, B.; Lin, X.; Bi, L.; Ma, R.; Tang, T. Influence of Land Use Change on Ecosystem Service Value Based on GEE in the Beijing-Tianjin-Hebei Region from 1998 to 2018. *Environ. Sci.* **2019**, *40*, 5473–5483.
56. Wang, B.; Ding, M.; Li, S.; Liu, L.; Ai, J. Assessment of landscape ecological risk for a cross-border basin: A case study of the Koshi River Basin, central Himalayas. *Ecol. Indic.* **2020**, *117*, 106621. [CrossRef]
57. Jiang, C. The 19th National Congress Report on the Development and Innovation of the Theory of Rule of Law in Socialism with Chinese Characteristics. *J. Shanghai Univ. Political Sci. Law (Rule Law Forum)* **2018**, *33*, 135–144.
58. Yan, Z.; Wang, Y.; Wang, Z.; Zhang, C.; Wang, Y.; Li, Y. Spatiotemporal Analysis of Landscape Ecological Risk and Driving Factors: A Case Study in the Three Gorges Reservoir Area, China. *Remote Sens.* **2023**, *15*, 4884. [CrossRef]
59. Hui, E.C.M.; Wu, Y.; Deng, L.; Zheng, B. Analysis on coupling relationship of urban scale and intensive use of land in China. *Cities* **2015**, *42*, 63–69. [CrossRef]
60. Yan, S.; Chen, W. Analysis of the decoupling state and driving forces of China's construction industry under the carbon neutrality target. *Environ. Sci. Pollut. Res.* **2022**, *29*, 78457–78471. [CrossRef]
61. Xia, H.; Ding, L.; Yang, S.; Wu, A. Socioeconomic factors of industrial air pollutants in Zhejiang Province, China: Decoupling and Decomposition analysis. *Environ. Sci. Pollut. Res.* **2020**, *27*, 28247–28266. [CrossRef]
62. Zhang, H.; Huang, Y.; Wang, R.; Zhang, J.; Peng, J. Decoupling and spatiotemporal change of carbon emissions at the county level in China. *Resour. Sci.* **2022**, *44*, 744–755. [CrossRef]

Disclaimer/Publisher's Note: The statements, opinions and data contained in all publications are solely those of the individual author(s) and contributor(s) and not of MDPI and/or the editor(s). MDPI and/or the editor(s) disclaim responsibility for any injury to people or property resulting from any ideas, methods, instructions or products referred to in the content.